International Journal of Biological Macromolecules 302 (2025) 140534

Contents lists available at ScienceDirect

International Journal of Biological Macromolecules

journal homepage: www.elsevier.com/locate/ijbiomac

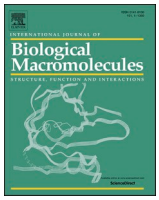

Lignin from aldehyde-assisted fractionation can provide light-colored Pickering emulsions through colloidal particles formed using alkaline antisolvent

Giovana Colucci [a,b,c], Andreia Ribeiro [b,c], Monique Bernardes Figueirêdo [d], Justine Charmillot [d], Arantzazu Santamaria-Echart [a], Alírio E. Rodrigues [b,c], M. Filomena Barreiro [a,*]

[a] CIMO, LA SusTEC, Instituto Politécnico de Bragança, Campus de Santa Apolónia, 5300-253 Bragança, Portugal
[b] LSRE-LCM – Laboratory of Separation and Reaction Engineering - Laboratory of Catalysis and Materials, Faculty of Engineering, University of Porto, Rua Dr. Roberto Frias, 4200-465 Porto, Portugal
[c] ALiCE – Associate Laboratory in Chemical Engineering, Faculty of Engineering, University of Porto, Rua Dr. Roberto Frias, 4200-465 Porto, Portugal
[d] Bloom Biorenewables, Route de l'Ancienne Papeterie 106, 1723 Marly, Switzerland

ARTICLE INFO

Keywords:
Lignin
Colloidal lignin particles
Pickering emulsions

ABSTRACT

Colloidal lignin particles (CLPs) are gaining attention as eco-friendly stabilizers for Pickering emulsions. Still, conventional lignin sources, like kraft lignin, are often limited by their dark color and strong odor. This study explores, for the first time, the use of a light-colored lignin derived from an aldehyde-assisted fractionation with glyoxylic acid (GA-lignin) for producing CLPs and derived Pickering emulsions. CLPs were produced by antisolvent precipitation with water (CLPs-W, pH 6) and alkaline buffer (CLPs-B, pH 8) as the antisolvents. The results revealed that the selected antisolvent significantly influenced the CLPs' properties. CLPs-W were larger, uniform in size, and hydrophobic, whereas CLPs-B were smaller, agglomerated into clusters, and exhibited greater hydrophilicity. Despite both CLPs' effectiveness in stabilizing oil-in-water emulsions, the stabilization mechanisms differed markedly; CLPs-W formed a robust membrane barrier at the oil-water interface, while CLPs-B facilitated oil droplet bridging. Overall, this work demonstrates that GA-lignin's light color nature offers advantages for Pickering emulsions design, surpassing a lignin typical limitation. This advancement highlights the versatility of GA-lignin-derived CLPs and supports the development of sustainable lignin-based products with significant commercial prospects.

1. Introduction

Conventional emulsions are dispersed systems consisting of two or more immiscible liquids stabilized by molecular compounds called surfactants. They are extensively applied in manufacturing commercial products across key industries, such as pharmaceuticals, cosmetics, and food [1]. However, using conventional molecular surfactants like polysorbates has been associated with adverse effects on human health, including allergies and endocrine disruption, as well as environmental issues such as water pollution and poor biodegradability [1–3]. Moreover, conventional emulsions exhibit thermodynamic instability, tending to break down over time [1,4]. From this perspective, Pickering emulsions, i.e., particle-stabilized emulsions, have been considered a more stable, safe, and sustainable alternative [5]. Indeed, the adsorption of solid particles at the oil-water interface confers a high resistance to coalescence, giving rise to highly stable systems [6]. Remarkably, Pickering emulsions stabilized using bio-based particles offer biological compatibility and eco-friendly characteristics, facilitating their application in diverse fields such as pharmaceuticals, cosmetics, drug delivery, and nutraceuticals [2,4].

Recent investigations have focused on using colloidal lignin particles (CLPs) for stabilizing Pickering emulsions [7–9]. Lignin is a biobased macromolecule consisting of a 3D-linked phenylpropane random network [10,11]. The presence of nonpolar aromatic moieties and polar hydroxyl groups in the same molecule and their rearrangement results in particles with a suitable wetting behavior, promoting their adsorption at oil-water interfaces [10,12]. Furthermore, the functional phenolic groups in the lignin structure confer remarkable properties such as

* Corresponding author.
E-mail address: barreiro@ipb.pt (M.F. Barreiro).

https://doi.org/10.1016/j.ijbiomac.2025.140534
Received 28 August 2024; Received in revised form 14 January 2025; Accepted 30 January 2025
Available online 31 January 2025
0141-8130/© 2025 The Authors. Published by Elsevier B.V. This is an open access article under the CC BY license (http://creativecommons.org/licenses/by/4.0/).

antioxidant, antimicrobial, and UV shielding. Thus, lignin and its derived particles can be considered multifunctional ingredients [8,11,13]. Pickering emulsions using CLPs have shown high potential for applications such as antimicrobials [14], oil recovery [15,16], anticancer drugs [17], food [18], and cosmetics [8,13]. Given the high versatility and potential of CLP-based Pickering emulsions, optimizing the CLP production process and understanding its impact on both the particles' properties and the stability of the resulting emulsions are crucial [13,19–23]. This understanding is essential for designing customized lignin-based Pickering emulsions that can effectively compete with conventional emulsions.

The antisolvent precipitation technique is widely applied to produce CLPs due to its simplicity, cost-effectiveness, controllable particle size, and morphology [24]. In this method, lignin is first dissolved in a suitable polar organic solvent (e.g., ethanol, acetone, or THF) and then added to an antisolvent. This addition causes the lignin to precipitate as CLPs due to its reduced solubility in the resulting mixture [24,25]. A suitable antisolvent must be miscible with the chosen organic solvent while not dissolving lignin. Water is the most commonly used antisolvent because of lignin's limited solubility, non-toxicity, and low-cost [24,26–28]. Selecting a suitable antisolvent is essential for forming and stabilizing the colloidal particles, which subsequently affects their final properties.

The pH of the antisolvent plays a vital role in particle formation and stabilization mechanisms, acting at the level of lignin electrostatic interactions and, thus, in its assembling behavior [25,29]. Leskinen et al. [27], who used NaOH aqueous solutions as the antisolvent to produce CLPs from kraft lignin, observed a size reduction of CLPs with pH increase due to the increased surface charge and electrostatic stabilization. Lignin agglomeration was reduced during particle formation, suggesting that high pHs allow the production of stable particles, even at higher lignin concentrations [27]. In agreement, in previous work of the group where kraft lignin-based CLPs [19] were produced using an alkaline phosphate-citrate buffer (pH 8), stable CLPs at a lignin concentration of 50 g/L were produced, resulting in excellent Pickering stabilizers. Therefore, high pH aqueous systems are advantageous for high-performance applications requiring high CLP concentrations.

The most commonly used lignin type in CLPs-based Pickering emulsions is kraft lignin, primarily due to its availability at the industrial scale [8,30–33]. However, kraft lignin's dark color and strong odor can pose challenges for its use in products where sensory quality is crucial, such as cosmetics. For this reason, functionalized lignins can be advantageous in meeting specific quality parameters for high-performance products such as Pickering emulsions. In this context, the aldehyde-assisted fractionation (AAF) process can be highlighted for producing uncondensed and highly pure lignins with a well-defined structure. They are achieved at extraction yields close to the maximum expected from the processed biomass, impacting economically the final products. Moreover, AAF-lignin extracted with glyoxylic acid (GA-lignin) is light-colored, an advantage over conventional lignins. This lignin has shown enhanced surface activity compared to kraft lignin, attributed to the controlled introduction of carboxylic acid groups and minimized condensation reactions [34]. Also, GA-lignin was successfully applied to produce high-transparency thermoset films with antioxidant properties and UV barrier activity [35]. The application of GA-lignin in Pickering stabilization has yet to be explored, and its light color, odorless nature, and functional properties make it an attractive option for developing healthcare products.

In this context, the present work focused on producing CLPs from GA-lignin and evaluating their Pickering performance. For CLPs production, ethanol aqueous solution was used to dissolve GA-lignin due to its green, biocompatible, and cost-effective aspects [26,36]. Water (the most used antisolvent) and alkaline buffer at pH 8 (an antisolvent showing promising results) were compared as antisolvents. The resulting CLPs were characterized in terms of their physicochemical and interfacial properties. These CLPs were then used to produce Pickering emulsions with varying oil volume fractions, and their microstructure and stability were examined. Finally, optimized emulsion formulations were characterized using confocal microscopy to gain insights into the stabilization mechanisms of CLPs. Also, the rheological behavior of the emulsions was accessed due to its importance in applications such as cosmetics.

2. Experimental

2.1. Materials

GA-lignin (from beech wood) obtained through aldehyde-assisted fractionation using glyoxylic acid [34] was kindly supplied by Bloom Biorenewables Ltd. (M_n = 1300 Da, M_w = 14,300 Da, 2.83 mmol/g aliphatic hydroxyl groups, 1.13 mmol/g phenolic hydroxyl groups, and 0.82 mmol/g carboxylic acid groups [35]). Ethanol absolute (purity ≥99.8 %) was purchased from Honeywell (Germany). Phosphate-citrate buffer solution (pH 8) with a molarity of 0.1 mol/L was prepared using di-sodium hydrogen phosphate anhydrous (Panreac, Spain) and citric acid (Merck, Germany). Miglyol 812 was purchased from Acofarma (Spain). Distilled water was used in all the processes.

2.2. Lignin solubility

The solubility of GA-lignin in 70 % ethanol aqueous solution (*v*/v) was determined for different concentrations (10, 30, and 50 g/L). Dried lignin was weighed in Eppendorf tubes, followed by solvent addition. The mixtures were left in an ultrasound bath for 30 min to ensure maximum solubilization. The solutions were centrifuged (ScanSpeed, Labogene, Denmark) at 13,500 rpm for 30 min. The supernatants were discarded, and the insoluble fractions were dried in an oven at 70 °C and weighed at room temperature.

2.3. CLPs production

CLPs were produced through the antisolvent precipitation method using a previously described group procedure [19] with minor modifications. Dried lignin was solubilized (30 g/L) in a 70 % ethanol aqueous solution (*v*/v) assisted by an ultrasound bath. The antisolvent was added to the lignin solution and kept under stirring at 500 rpm, at a controlled flow rate (14 mL/min), using a syringe pump (KDS 200, KD Scientific, USA). The amount of antisolvent added was calculated to achieve a final ethanol concentration of 45 % (*v*/v). Pure distilled water (pH 6), further designated as water, was used to produce CLPs-W, and phosphate-citrate buffer (pH 8) produced CLPs-B. In the final step, the solvent (ethanol plus some water) was removed in a rotary evaporator (R-114, Waterbath B-480, and Vacuum Controller B-721, Büchi, Switzerland) at 60 °C under reduced pressure to achieve the same initial lignin concentration (30 g/L). The final lignin concentration was checked gravimetrically by drying an aliquot of the dispersion to constant weight. CLPs were stored at room temperature and protected from light to prevent possible photodegradation effects.

2.4. Pickering emulsions production

Pickering emulsions PE-W and PE-B were produced from CLPs-W and CLPs-B, respectively, according to a procedure described elsewhere [37] with minor modifications. Miglyol 812 was added dropwise to the CLPs dispersion and kept under stirring (13,500 rpm) with a rotor-stator homogenizer (CAT, Unidrive X 1000, Germany). After complete oil addition, the emulsion was further homogenized for 5 min. Emulsions of different oil volume fractions (Φ = 0.4, 0.5, 0.6, 0.7, and 0.8) were prepared using CLPs at a fixed lignin concentration (30 g/L) in the aqueous phase. Emulsions were stored at room temperature and protected from light to prevent possible photodegradation effects.

2.5. Size and zeta potential

The size of CLPs and emulsion droplets was measured using a Mastersizer 3000 equipped with a Hydro MV dispersion unit (Malvern Instruments Ltd., United Kingdom). The refractive index and absorption of GA-lignin were set to 1.6 and 0.1, respectively, based on published data [38,39], as these values provided the best fit for the observed particle size distributions, following the recommended procedure for samples with unknown parameters. Samples were added as such in the dispersing media (distilled water) until achieving an obscuration of about 3.5 % (CLPs) or 7 % (emulsions) and analyzed at room temperature, averaging 5 measurements. The CLPs particle size was characterized by the D50, the median diameter where 50 % of particles are smaller, by number and volume. Emulsion droplet size was represented by the $D_{4,3}$ volume-weighted mean diameter, also known as De Brouckere mean diameter.

The width of the size distribution was determined by the span value (Eq. (1)).

$$Span = \frac{D_{90} - D_{10}}{D_{50}} \quad (1)$$

where D_{90} and D_{10} are the sizes below 90 % and 10 % of the sample, respectively, and D_{50} is the median size.

The CLPs surface charge was determined by particle electrophoresis using a Nano-ZS Zetasizer instrument (Malvern Instruments Ltd., United Kingdom) equipped with a standard DTS1070 disposable folded capillary cell. CLPs were diluted at a 1:30 (*v*/v) ratio in distilled water. Results are expressed as the average of 3 measurements at 25 °C.

2.6. CLPs interfacial properties

The interfacial properties comprised the determination of the three-phase contact angle (θ_{ow}) and the interfacial tension. The sessile drop method was used to determine θ_{ow}, representing the angle between the CLP surface and the tangent to the oil-water interface. For this, CLPs were dried and used to produce tablets with a diameter of 13 mm and a thickness of circa 3 mm using a hydraulic press (Specac Ltd., United Kingdom). The pellets' surface was checked by optical microscopy (Nikon Eclipse 50i, Nikon Corporation, Japan) to discard the ones with surface cracks. For the measurement, CLP tablets (triplicate) were placed in a quartz cuvette filled with Miglyol 812 (30 mL), followed by the deposition of a water drop (5 μL) on its surface. The θ_{ow} was recorded by a camera coupled to the goniometer (model 210, Ramé-Hart Instrument Co., USA) after 30 s of the drop deposition. The pendant drop method was applied to measure the interfacial tension of the systems (water-oil, CLPs-W-oil, and CLPs-B-oil). For this, a drop (20 μL) of water or CLPs dispersion was formed by a submerged syringe inside the cuvette filled with Miglyol 812 (30 mL). The interfacial tension was calculated over 2000 s using the equipment software. Experiments were conducted at room temperature.

The energy of desorption (E_D) in Joule was calculated according to Eq. (2) [40]:

$$E_D\ (J) = \pi r^2 \gamma_{ow}(1 \pm cos\theta_{ow})^2 \quad (2)$$

where r is the particle radius ($D_{50}/2$ in number), γ_{ow} is the water-oil interfacial tension, and θ_{ow} is the three-phase contact angle between the solid particle, oil, and water.

2.7. CLPs morphology

Transmission electron microscopy (TEM) was used to analyze the morphology of the particles. CLPs were diluted at a 1:200 (*v*/v) ratio with distilled water, and 10 μL was dropped on Formvar/carbon film-coated mesh nickel grids (Electron Microscopy Sciences, USA) and left standing for 2 min. The excess liquid was removed with filter paper. Visualization was conducted by a JEM-1400 Flash Electron Microscope (JEOL Ltd., Japan) at 120 kV, and the images were acquired using a CCD digital camera Orious 1100 W (Japan).

2.8. Emulsion morphology and microstructure

Emulsion morphology and microstructure were checked by optical microscopy using a Nikon Eclipse 50i microscope (Nikon Corporation, Japan) equipped with a Nikon Digital camera. Sample aliquots (emulsified phase) were placed on a microscope slide and covered with a coverslip. Image acquisition (200× magnification) and processing were performed using NIS-Elements Documentation software.

The interfacial microstructure of the formed droplets was analyzed by confocal microscopy (Leica TCS-SP5 AOBS, Leica Microsystems Inc. Heidelberg, Germany). Emulsion samples were placed on concave slides, and lignin autofluorescence was inspected using an argon laser (excitation at 488 nm and emission at 495–608 nm). Images were acquired with a 63× oil immersion objective.

2.9. Emulsion stability parameters

The emulsion macroscopic and microscopic stability was assessed by determining the formed emulsified layer (EL) and the emulsion instability index (EII), respectively. EL was determined according to Eq. (3) [19]:

$$EL\ (\%) = \frac{H_E}{H_T} \times 100 \quad (3)$$

where H_E is the height of the emulsified layer, and H_T is the total height of the sample placed in a flat vial. The EL was measured after 1, 7, 15, and 30 days of sample storage. EII was calculated according to Eq. (4) [41]:

$$EII = \frac{d(t) - d(0)}{d(0) \times t} \quad (4)$$

where d(0) is the initial droplet diameter, and d(t) is the droplet diameter at time t. In this work, d(0) and d(t) correspond to the emulsion mean droplet size $D_{4,3}$ after 1 and 30 days of storage, respectively.

2.10. Emulsion type

The drop test was used to confirm the emulsion type. Three emulsion drops were added to individual beakers, one containing water and the other containing Miglyol 812 oil. After gentle stirring, the emulsion type was determined based on the observed dispersing behavior. If the emulsion drops rapidly disperse in water and remain intact in the oil, the emulsion is classified as oil-in-water (O/W) type. Conversely, if the drops disperse in the oil and remain intact in the water, it is classified as a water-in-oil (W/O) type. The principle of the method is that the drops disperse in the liquid corresponding to their external phase [42].

2.11. Emulsion rheology

The viscous and viscoelastic behavior of emulsions was analyzed using a parallel plate (PP50) rheometer (MCR 92, Anton Paar, GmbH, Austria) with a gap size of 1 mm at 25 °C. The dynamic viscosities were determined as a function of the shear rate in the 0.1 to 1000 1/s range. The frequency sweep oscillated from 100 to 0.03 rad/s, and all measurements were performed within the determined linear viscoelastic region (LVE) at a 0.1 % strain. Data is reported as storage modulus (G') and loss modulus (G'') as a function of frequency.

3. Results and discussion

3.1. CLPs production

According to solubility tests conducted with a 70 % ethanol aqueous solution (*v*/v), GA-lignin at a concentration of 30 g/L exhibited a 97 % soluble fraction, making it suitable for proceeding with CLPs production following the antisolvent precipitation method. Accordingly, the overall higher water affinity of this lignin type (due to the functionalization with carboxyl groups) is beneficial for its solubility in ethanol. The impact of using water versus the alkaline buffer (pH 8) antisolvents on CLPs formation was inspected by analyzing the visual appearance of the dispersions, the size distribution, and the morphology of the particles (Fig. 1). CLPs-W had a narrow size distribution translated by low span values and a close median diameter in number and volume, revealing a high homogeneity (Table 1). They presented well-defined and uniform spherical shapes of dense structure (Fig. 1c). CLPs-B comprised predominantly small-sized particles, as seen by their median diameter in number (Table 1), yet forming agglomerates as perceived by the broad distribution in volume (Fig. 1e). Accordingly, the TEM images (Fig. 1f) revealed that CLPs-B had an irregular shape and tended to form clusters, yet small and isolated particles of light grey color can be perceived revealing a less dense structure compared to CLPs-W. In addition, the light and white spots observed in Fig. 1f can be due to small and spherical agglomerates of CLPs under specific conditions of TEM analysis, which are usually associated with poor staining (when applied), low concentration, or thin layers.

The zeta potential of the CLPs was measured as an indicator of their surface charge and electrical double-layer repulsion [36]. Both CLPs exhibited a high negative surface charge (Table 1), which can be correlated to the content of acidic groups in lignin, such as phenolic hydroxyl and carboxyl groups, and partly to the adsorption of hydroxyl ions [38,43]. In this way, GA-lignin resulted in highly stable CLP dispersions produced by the antisolvent precipitation method, independently of the used antisolvent.

CLPs-W showed a light pastel orange color and opaque aspect, whereas CLPs-B showed an orangish hue with a translucent aspect. The distinct characteristics of CLPs-W and CLPs-B and the visual aspect of the dispersions along the production stages (Fig. S1) pointed out differences in CLPs formation linked to the used antisolvent. In fact, the formation of

Table 1
Median particle size and span in number and volume, and zeta potential of CLPs.

	Size (nm)		Span		Zeta potential (mV)
	Number	Volume	Number	Volume	
CLPs-W	392 ± 3	494 ± 5	0.7	0.8	−60 ± 1
CLPs-B	172 ± 1	581 ± 6	1.1	6.3	−66 ± 3

CLPs using the antisolvent precipitation technique relies on the changing solubility of lignin at different stages due to the addition of the antisolvent. During this process, lignin precipitates according to a molecular weight (MW) dependent pattern [26]. Considering this fact and the experimental observations, it can be hypothesized that in the CLPs-W, the addition of water (antisolvent) quickly led to lignin supersaturation in the solution due to its poor solubility in water. This caused the precipitation of most lignin fragments, ranging from high to low MW, into well-defined spherical forms to minimize the surface area in contact with water. During ethanol removal, the solubility of lignin further decreases, causing the small polar lignin fragments still in solution to adsorb onto the already formed particles, thereby increasing the particle size [26]. In contrast, alkaline antisolvent drives the deprotonation of carboxyl groups of lignin ($pK_a \sim 4.7$), increasing the solubility of lignin molecules in the aqueous medium [10,27]. Therefore, in the production of CLPs-B, the supersaturation condition for lignin precipitation is reached at later stages. This indicates that only the high MW lignin fragments precipitated during antisolvent addition, while the smaller ones, which are more polar, remained in the solution even after ethanol removal.

The final pH of CLPs-W and CLPs-B was 3.4 and 5.3, respectively. The functionalization of GA-lignin with carboxylic acid groups integrated into its structure imparted a more acidic character to the CLPs, indicating a greater water affinity at pH levels above the pK_a of 4.7 [34,35]. This confirms that some lignin molecules, particularly the ones with higher polarity, remained soluble in the case of CLPs-B. The absence of these polar groups on the CLPs-B surface contributed to particle agglomeration, as observed in TEM images.

3.2. CLPs as Pickering stabilizers

The interfacial properties of CLPs are crucial in determining their

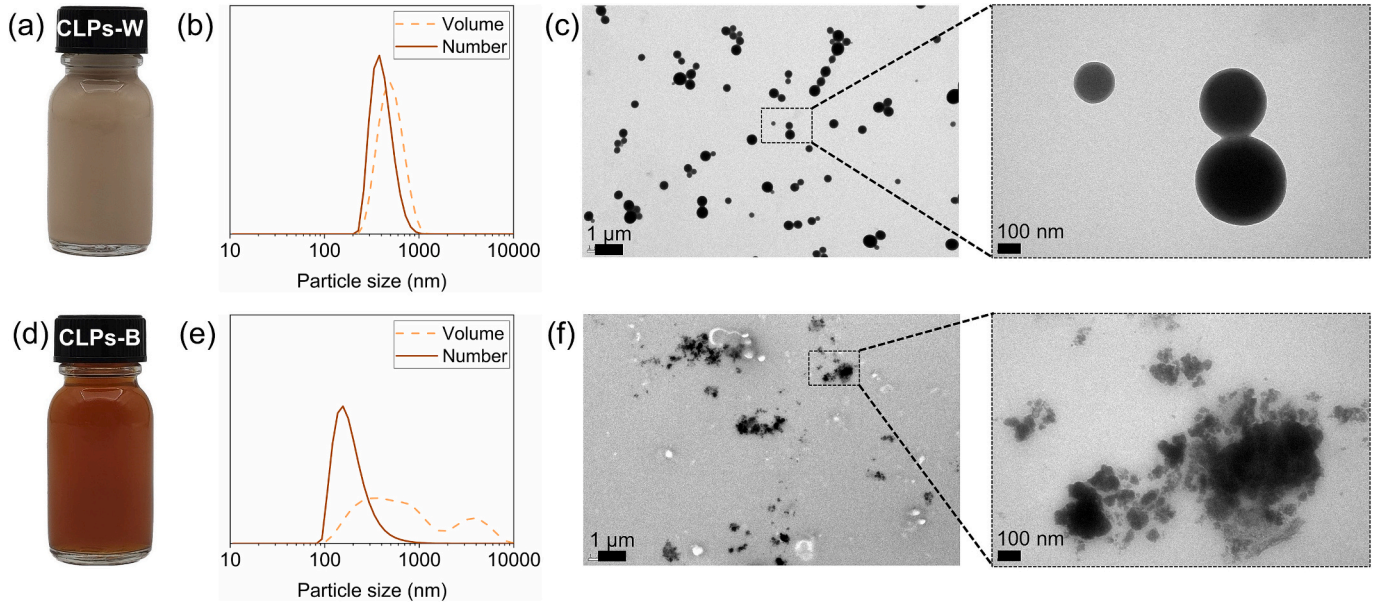

Fig. 1. Digital images, size distributions, and TEM images of CLPs-W (a, b, and c) and CLPs-B (d, e, and f), respectively. TEM magnifications of 12,000 (left) and 100,000× (right).

effectiveness as Pickering stabilizers. For particles to be adsorbed at the oil-water interface, a precondition to be observed is that they must be partially wetted by both the oil and water phases [44]. The three-phase contact angle (θ_{ow}) indicates the degree of wettability of the particles and determines the type of emulsion they will stabilize [44,45]. For closely packed particles and particles with 3D networks, a θ_{ow} value between 15° and 129.3° can effectively stabilize oil-in-water (O/W) emulsions. In contrast, values between 50.7° and 165° are appropriate to stabilize water-in-oil emulsions (W/O) [9,45]. The emulsion type formed at the overlapping interval (50.7°-129.3°) depends on the oil volume fraction (ϕ) and preparation conditions [4,45]. At θ_{ow} values outside these ranges, the particles are either too hydrophilic (close to 0°) or too hydrophobic (close to 180°) to be adsorbed at the oil-water interface [45]. CLPs-W exhibited a more hydrophobic character (Fig. 2a) compared to CLPs-B (Fig. 2b) due to the different arrangement of lignin functional groups on the CLPs' surface, a feature resulting from the used antisolvent. Nevertheless, both CLPs exhibited θ_{ow} values within the required range to effectively stabilize emulsions. Moreover, Fig. 2c shows the interfacial tension of CLP suspensions and oil compared to water and oil, revealing that both CLPs reduced the interfacial tension, indicating that particles migrated to the oil-water interface and were adsorbed [5].

To estimate how strong the CLPs adsorb at the oil-water interface, the energy of desorption (E_D), i.e., the energy required to remove the particle from the interface, was calculated (Eq. (2)). Table S1 shows the parameters used to calculate E_D and Table 2 lists the estimated E_D of CLPs, in units of thermal energy k_BT, compared with literature data. CLPs-W presented a higher E_D value than CLPs-B, mainly attributed to its larger particle size, considering its quadratic effect (r^2) on E_D. Both CLPs presented very high E_D values, on the order of 10^5 and 10^4 k_BT, indicating that the energy required to remove a particle from the interface far exceeds thermal fluctuations or Brownian motion [46]. Therefore, the CLPs can be considered irreversibly adsorbed at the oil-water interface [40,46]. In fact, the E_D values of both CLPs were similar to or superior to those of other lignin particle-oil systems reported in the literature, emphasizing the high adsorption properties of the prepared GA-lignin-derived CLPs in the resulting Pickering systems.

Table 2
The energy of desorption (E_D) of CLPs at the oil-water interface compared to literature.

Lignin particle	Oil	E_D (k_BT)	Reference
CLPs-W	Miglyol	9.8×10^5	This study
CLPs-B	Miglyol	2.8×10^4	This study
N-SEKL[a] (pH 3)	Xylene	6.0×10^5	[22]
LNPs[b]	Thyme	1.0×10^4	[47]
KLP[c] (pH 11)	Soybean	7.0×10^2	[10]
KLP (pH 7)	Soybean	2.8×10^4	
KLP (pH 2)	Soybean	2.8×10^6	
F_0-KLP	Sunflower	1.0×10^2	[9]
F_1-KLP	Sunflower	2.5×10^0	
F_2-KLP	Sunflower	4.6×10^3	
F_3-KLP	Sunflower	2.0×10^2	

[a] N-SEKL: sulfoethylated lignin nanoparticles.
[b] Lignin nanoparticles.
[c] Kraft lignin particles.

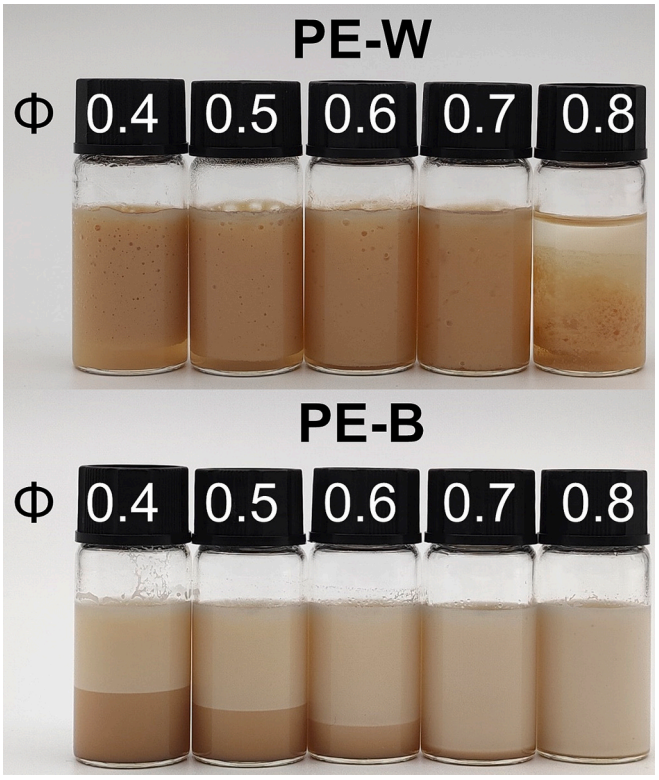

Fig. 3. Visual appearance of PE-W and PE-B Pickering emulsions prepared with different oil volume fractions (Φ) after 1 day of storage.

3.3. Characterization of Pickering emulsion systems

Pickering emulsions PE-W and PE-B were obtained using CLPs-W and CLPs-B, respectively. Fig. 3 shows a digital image of the formulations produced with varied volumes of the dispersed oil phase (Φ = 0.4, 0.5, 0.6, 0.7, and 0.8), highlighting the differences between PE-W and PE-B regarding color and visual appearance 1 day after their preparation. The complete register considering 1, 7, 15, and 30 days of storage is included in Fig. S2. The PE-W emulsions exhibited light pastel shades of orange, reflecting the color of CLPs-W, while the PE-B emulsions displayed light white tones due to the translucent nature of CLPs-B. Indeed, the light brown color of GA-lignin is a notable advantage in the production of

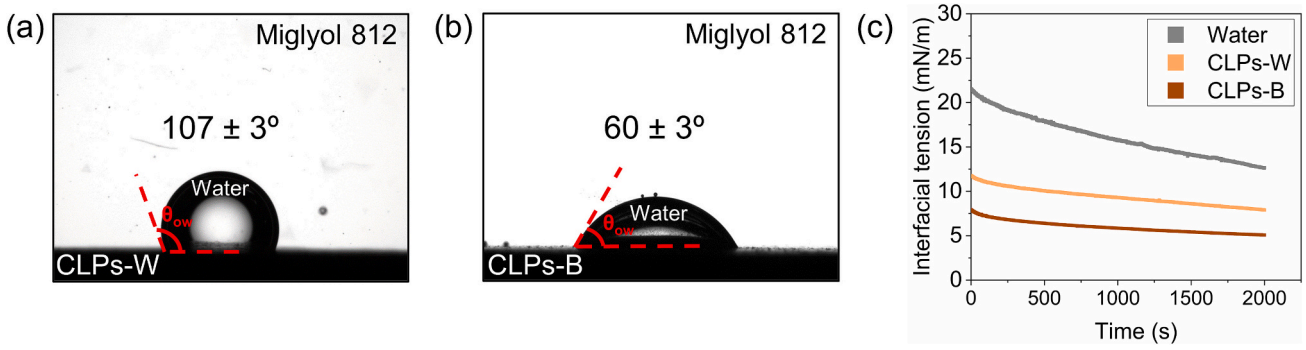

Fig. 2. Three-phase contact angle θ_{ow} of (a) CLPs-W and (b) CLPs-B and (c) interfacial tension between oil (Miglyol 812) and water or CLPs.

light color lignin-based emulsions when compared to Pickering emulsions produced with kraft-lignin-derived CLPs [8,31,33], which present dark brown tones and have limited application in products requiring light color, such as cosmetic formulations. Moreover, the drop test revealed that all emulsions were O/W type.

Regarding the effect of Φ on emulsion droplet size, for PE-W formulations, the droplet size ($D_{4,3}$) increased as Φ increased (Table 3). Indeed, at a fixed particle concentration, an increase in Φ reduces the number of particles available to stabilize the increased interfacial area, forming larger droplets [4]. This behavior was commonly reported for Pickering emulsion systems [15,37,48,49]. For a Φ of 0.8, emulsion disruption occurred due to the high oil content exceeding the particles' capacity to stabilize the system. For this reason, this formulation was not characterized. In contrast, increasing Φ in PE-B formulations led to a droplet size decrease. In this case, the distribution of CLPs-B in the emulsion structure and their stabilization mechanism led to this opposite droplet size effect, which will be discussed in more detail in Section 3.4. The impact of Φ on emulsion droplet size is also visually evident in the optical microscopy images of the formulations (Fig. 4).

Differences in the magnitude of the droplet size were observed for PE-W and PE-B, i.e., the droplets formed in the PE-W formulations were larger than in the PE-B ones (Fig. 4), independently of the used Φ. In fact, the droplet size of Pickering emulsions is influenced by the size of the stabilizing particles [1], with the emulsion droplet size increasing with particle size increase. This is mainly because larger particles take a longer time to adsorb at the interface during emulsion formation, resulting in larger emulsion droplets [1,4]. This aligns with the obtained results, where CLP size directly influenced the size of the resulting emulsion droplets. Regarding morphology, both emulsion formulations exhibited spherical droplets regardless of the used Φ.

The stability of the Pickering emulsions was analyzed according to two parameters, namely, the formed emulsified layer (EL) over storage time and the emulsion instability index (EII). The EL translates the particles' ability to form and hold an emulsion layer over storage, varying from 0 (EL not formed) to 100 % (wholly emulsified system) [19]. Fig. 5a and b show the calculated EL of PE-W and PE-B formulations, respectively. Most formulations achieved a constant EL after 7 days of storage. This is commonly observed in Pickering emulsion systems, as particles require some equilibrium time after emulsification to achieve the full coverage of the oil-water interface [6]. This means that, after the equilibrium period, CLPs could hold the oil droplets for at least 30 days of storage. Furthermore, the impact of the Φ in EL is observed, where for both emulsion types, the EL increased as Φ increased (except for PE-W at Φ = 0.8, where EL was equal to 0). The observed result evidences the high emulsifying capacity of CLPs-W and CLPs-B, revealing their ability to stabilize large oil volumes.

The EII is linked to the emulsion microscopy stability, as it translates the rate of droplet size change over time. Thus, its value increases as instability increases due to droplet aggregation [41]. In this study, the EII was estimated by comparing the droplet size of the emulsions after 1 and 30 days of storage. All formulations presented an EII equal to or lower than 0.01 (Table 3); thus, they were considered highly stable [41].

Table 3
Emulsion volume mean droplet size ($D_{4,3}$) and emulsion instability index (EII) of PE-W and PE-B prepared with different oil volume fractions (Φ).

Φ	PE-W			PE-B		
	$D_{4,3}$ (Day 1)	$D_{4,3}$ (Day 30)	EII	$D_{4,3}$ (Day 1)	$D_{4,3}$ (Day 30)	EII
0.4	42.0 ± 0.1	43.0 ± 0.2	0.00	17.0 ± 0.5	19.3 ± 0.1	0.00
0.5	58.3 ± 0.1	57.7 ± 0.1	0.00	15.6 ± 0.1	18.1 ± 0.1	0.01
0.6	78.0 ± 0.6	81.8 ± 0.6	0.00	13.1 ± 0.1	15.7 ± 0.2	0.01
0.7	91 ± 2	89 ± 3	0.00	13.4 ± 0.1	14.2 ± 0.6	0.00
0.8	-	-	-	7.0 ± 0.1	7.4 ± 0.1	0.00

- Not determined.

In addition, no significant changes were observed in the emulsions' microstructure until 30 days of storage (Fig. S3).

The PE-W at Φ = 0.7 (PE-W-0.7) and PE-B at Φ = 0.8 (PE-B-0.8) exhibited an EL equal to 100 % over 30 days of storage and EII equal to 0, revealing promising long-term stability. For this reason, they were selected as the optimized formulations to conduct the additional analyses of this study. The drop test was registered in these formulations to prove their O/W type (Fig. S4).

3.4. Stabilization mechanism of Pickering emulsions by CLPs

The unique characteristics of PE-W and PE-B suggest different stabilization mechanisms. To verify this hypothesis, the interfacial structures of Pickering emulsions (PE-W-0.7 and PE-B-0.8) were examined using confocal laser scanning microscopy (CLSM), utilizing the autofluorescence of lignin to observe the distribution of colloidal lignin particles (CLPs) within the emulsions (Fig. 6). The CLSM images revealed that CLPs-W were distributed around the oil droplets' surface, as perceived by the presence of an intense green halo around them (Fig. 6a). Additionally, the droplets were dispersed individually. Due to their greater hydrophobicity and affinity for the oil phase, CLPs-W were strongly adsorbed at the oil-water interface. These observations suggest that PE-W-0.7 was mainly stabilized by the typical stabilization mechanism called interfacial membrane barrier, in which particles are strongly adsorbed at the oil-water interface, forming a sufficiently dense layer that provides steric hindrance and consequently prevents droplet coalescence and interaction [1,50].

When using CLPs-B, the oil droplets were sparsely covered (Fig. 6b), with the particles becoming distributed in the continuous phase. Besides, tightly packed oil droplets were observed. This suggests that PE-B-0.8 was mainly stabilized by the bridging mechanism, where a network of particles in the aqueous phase connects the droplets [1]. In this mechanism, tightly packed oil droplets are stabilized by a shared particle monolayer network that exerts strong adhesive forces, preventing droplets from aggregating [51]. Indeed, as pointed out by French et al. [52], essential prerequisites for bridging include a high affinity of the particles with the continuous phase (CLPs-B have a hydrophilic character), together with a large interfacial area generated during the homogenization process (a high number of oil droplets were formed in the PE-B formulations regardless the Φ). Moreover, the presence of soluble lignin molecules in CLPs-B can also have positive effects, as it contributes to emulsion stability as a molecular surfactant [34]. In fact, Hadjiefstathiou et al. [20] found a synergic effect between lignin particles and lignin surfactant molecules, resulting in enhanced interfacial stabilization of O/W emulsions. Furthermore, Tian et al. demonstrated a synergistic stabilization mechanism in Pickering emulsions by using lignin solid particles in combination with lignin-based hydrocolloids [10]. In this work, the PE-B stabilization could be attributed to the simultaneous adsorption of CLPs and solubilized lignin molecules at the oil-water interface. This can explain the distinct behavior of PE-B formulations for different Φ values (Section 3.3), where the droplet size decreased as Φ increased. In fact, the presence of lignin surfactant molecules in CLPs-B further reduced the interfacial tension between oil and water (Fig. 2c) [20], contributing to an increase in the interfacial area as the Φ increased [41]. This combined mechanism enabled a more efficient packing of the oil droplets, allowing O/W emulsions to be effectively stabilized even at a Φ of 0.8.

3.5. Rheology of Pickering emulsions

The rheological behavior of Pickering emulsions is related to their structure, composition, and physical stability [37,50]. The presence of particles significantly impacts emulsion rheology due to interparticle interactions. Namely, emulsions with a sufficiently high concentration of particles display non-Newtonian and viscoelastic behaviors [50]. The emulsions presented a thick aspect (Fig. 7a and b) and showed typical

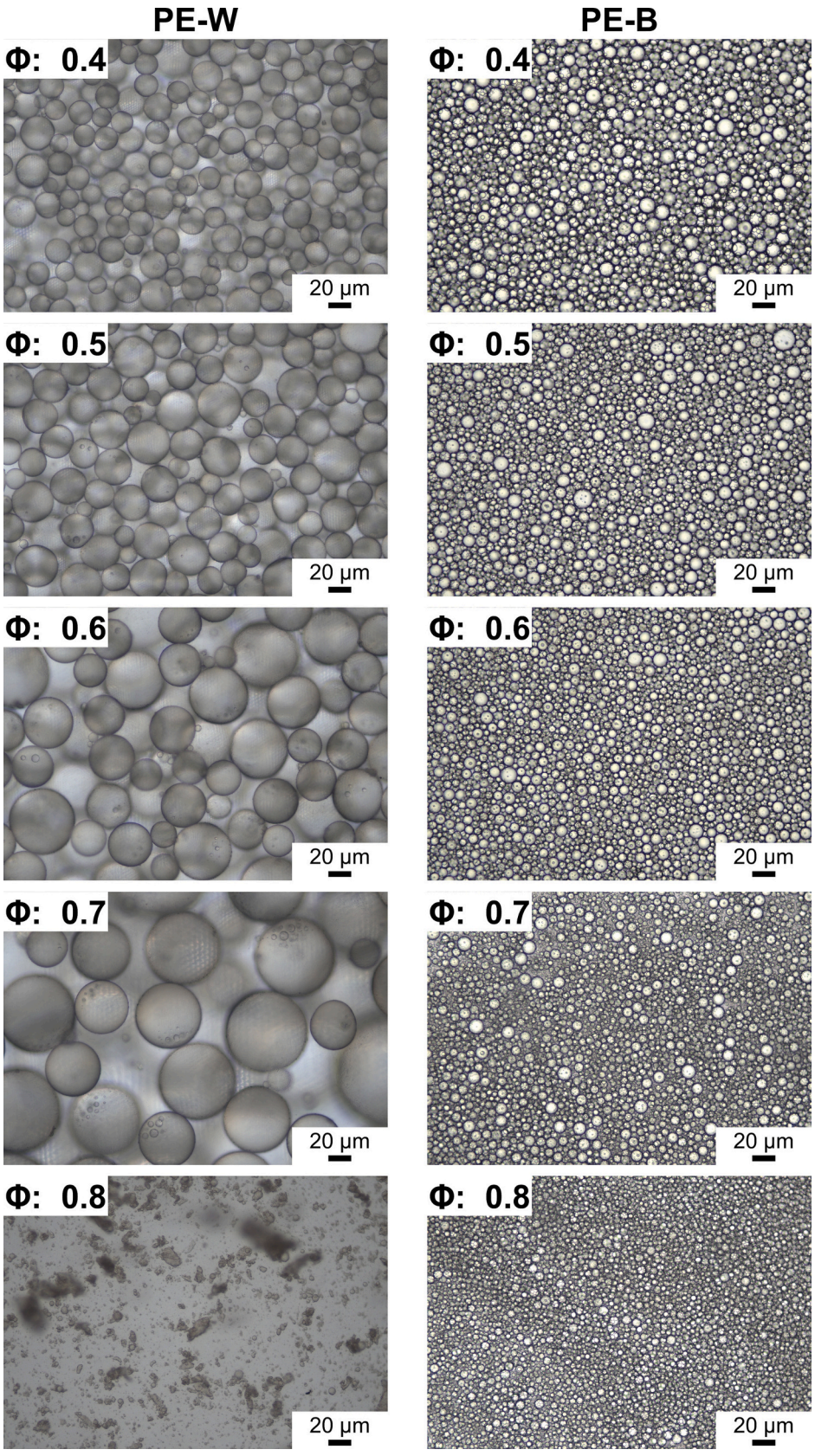

Fig. 4. Microscopic images of Pickering emulsions prepared with different oil volume fractions (Φ) after 1 day of storage.

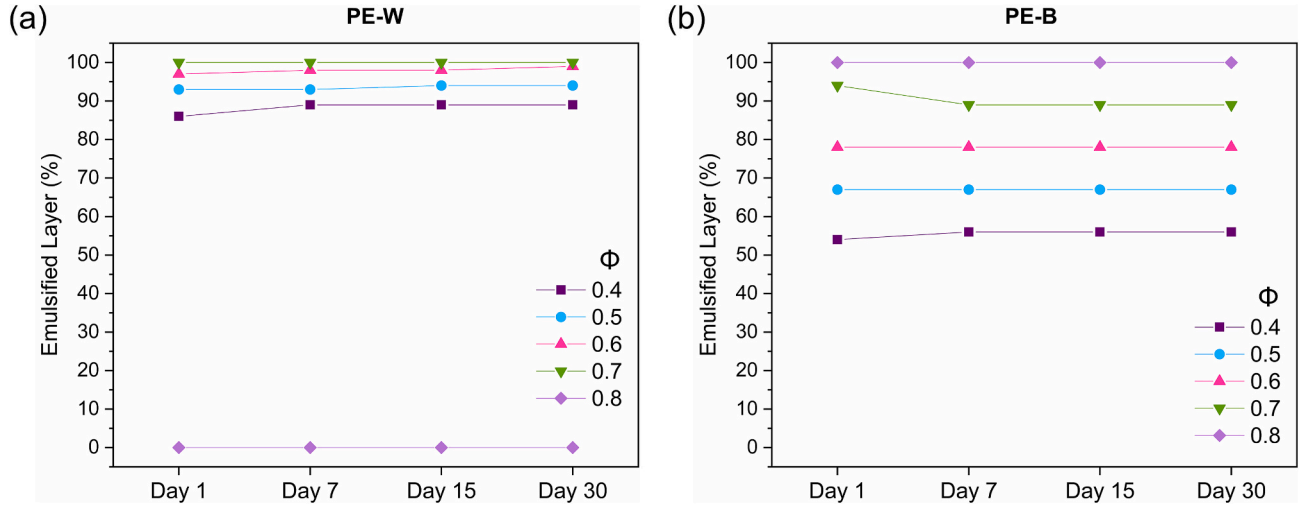

Fig. 5. Emulsified layer (EL) over storage time of (a) PE-W and (b) PE-B formulations prepared with different oil volume fractions (Φ).

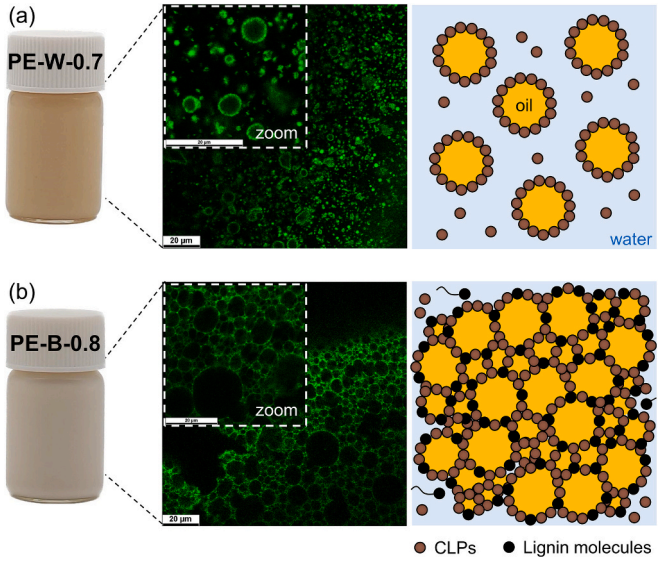

Fig. 6. Visual aspect, confocal microscopy images, and illustration of the proposed stabilization mechanism of PE-W-0.7 (a) and PE-B-0.8 (b).

non-Newtonian, shear-thinning behavior, i.e., the increase of the shear rate decreases their viscosity (Fig. 7c) [53]. The decrease in viscosity with applied force facilitates spreading into the skin, a desirable and essential attribute for cosmetic creams [54].

Frequency sweep tests were also conducted (Fig. 7d) to determine the storage modulus (G′) and the loss modulus (G″), which correspond to the emulsions' elastic and viscous behavior, respectively [53]. In both formulations, G′ was higher than G″ for the applied angular frequency, revealing their elastic behavior. This indicates that the emulsions exhibit gel-like structures because of stable forces network, providing mechanical stability at rest [53].

PE-B-0.8 exhibited a higher G' (almost 10 times) and a firmness texture (visual observation) than PE-W-0.7. In fact, the higher Φ value and the associated stabilizing mechanism influenced the obtained results. In accordance, Lee et al. [51], in a rheological study dealing with Pickering emulsions stabilized with silica particles, attributed firmer gel-like behavior to the bridging particles stabilization mechanism. As for the PE-B-0.8 formulation, where oil droplets were densely packed and CLPs were mainly distributed in the aqueous phase, higher G′ values were observed, suggesting a higher resistance to deformation [37]. Compared with an O/W emulsion cosmetic cream prepared with a synthetic polymer (polyacrylamide) [55], PE-B-0.8 exhibited similar flow behavior and viscosity, highlighting its potential to be explored in this field.

4. Conclusions

The current study demonstrated that GA-lignin is a viable alternative to traditional industrial lignins known for their dark brown color, such as the case of kraft lignins. This substitution leads to lighter-colored Pickering emulsions, which align with the cosmetic industry's aesthetic preferences. According to the developed process, the specific type of antisolvent influences the properties and stabilization mechanisms of GA-lignin-based CLPs. Both CLPs prepared with water and the alkaline antisolvent stabilized O/W Pickering emulsions, offering excellent long-term stability yet resulting in GA-lignin-based Pickering emulsions with distinct properties.

The optimized emulsion produced with the alkaline antisolvent (PE-B-0.8) exhibited a favorable light color and creamy texture, making it a promising formulation for cosmetic applications. Moreover, the odorless nature of GA-lignin represents a significant advantage for product development. However, further validation is necessary to ensure safety, efficacy, and compliance with regulatory standards. Overall, this study offers new insights into lignin-based formulations, emphasizing the role of CLPs in stabilizing Pickering emulsions and highlighting the potential of functionalized lignins, such as GA-lignin, in commercial products requiring specific sensory attributes, like light color, representing a step forward in lignin valorization.

CRediT authorship contribution statement

Giovana Colucci: Writing – review & editing, Writing – original draft, Validation, Methodology, Investigation, Formal analysis, Conceptualization. **Andreia Ribeiro:** Methodology, Investigation. **Monique Bernardes Figueirêdo:** Writing – review & editing, Conceptualization. **Justine Charmillot:** Writing – review & editing, Conceptualization. **Arantzazu Santamaria-Echart:** Writing – review & editing, Methodology. **Alírio E. Rodrigues:** Writing – review & editing, Supervision. **M. Filomena Barreiro:** Writing – review & editing, Supervision, Resources, Project administration, Funding acquisition, Conceptualization.

Declaration of competing interest

The authors declare that they have no known competing financial

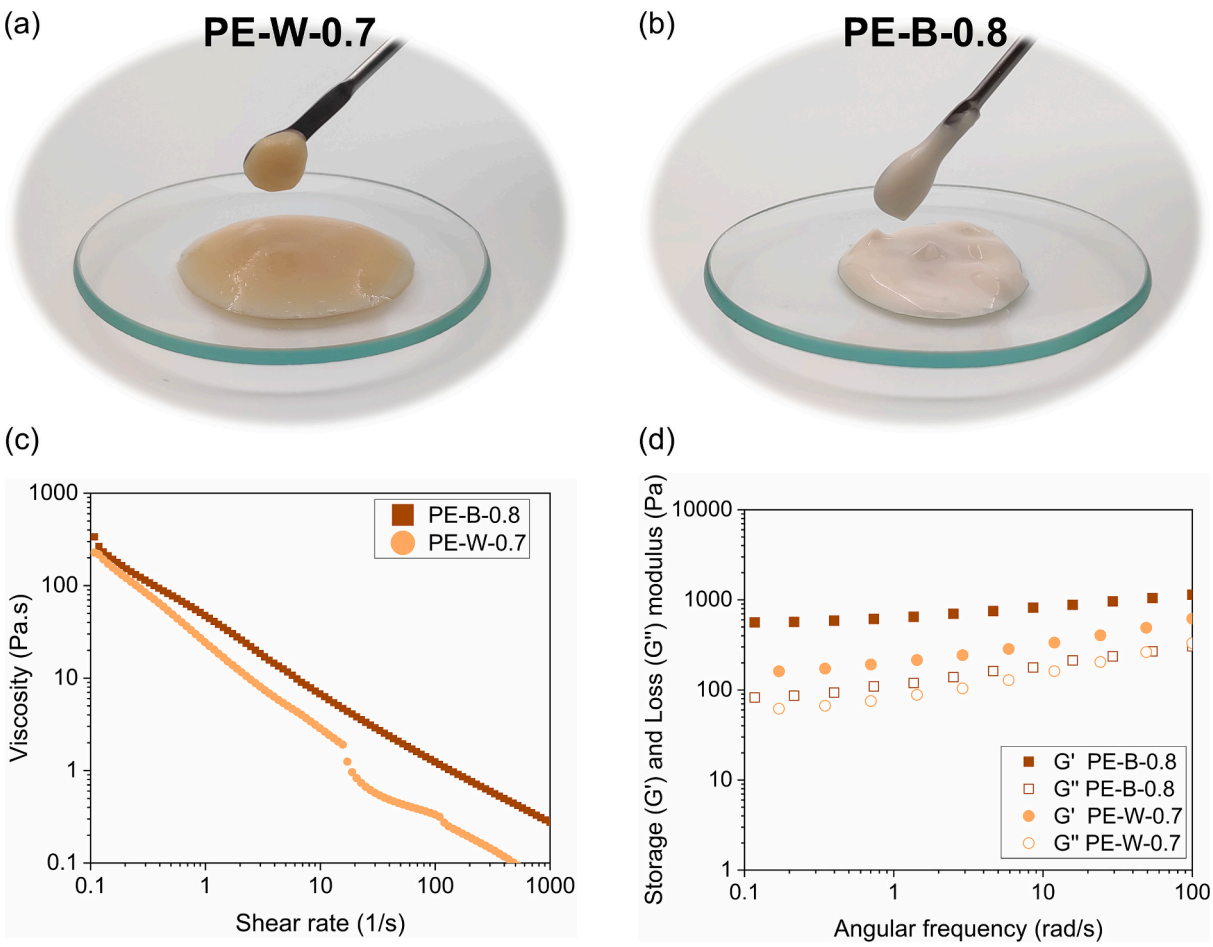

Fig. 7. Rheology of Pickering emulsions: spatula observation of (a) PE-W-0.7 and (b) PE-B-0.8, (c) apparent viscosity versus shear rate, and (d) storage (G′) and loss (G″) modulus versus angular frequency.

interests or personal relationships that could have appeared to influence the work reported in this paper.

Acknowledgments

The authors are grateful to the Foundation for Science and Technology (FCT, Portugal) for financial support through national funds FCT/MCTES (PIDDAC) to CIMO UIDB/00690/2020 (10.54499/UIDB/00690/2020) and UIDP/00690/2020 (10.54499/UIDP/00690/2020); SusTEC LA/P/0007/2020 (10.54499/LA/P/0007/2020); LSRE-LCM UIDB/50020/2020 (10.54499/UIDB/50020/2020) and UIDP/50020/2020 (10.54499/UIDP/50020/2020); and ALiCE LA/P/0045/2020 (10.54499/LA/P/0045/2020). FCT for the Ph.D. research grant of G. Colucci (2021.05215.BD). FCT for the institutional scientific employment program contract of A. Santamaria-Echart and the research contract of A. Ribeiro (CEEC, 10.54499/2022.00798.CEECIND/CP1733/CT0009). M. B. Figueirêdo acknowledges the European Union's Horizon 2020 research and innovation program under the Marie Skłodowska-Curie Grant Agreement No.: 101032664. J. Charmillot acknowledges the Swiss State Secretariat for Education, Research and Innovation through the "VALORISE" project (SBFI No. MB22.00005/REF-1131-52105). i3s Scientific Platform HEMS for the technical support.

Appendix A. Supplementary data

Supplementary data to this article can be found online at https://doi.org/10.1016/j.ijbiomac.2025.140534.

References

[1] L. Ming, H. Wu, A. Liu, A. Naeem, Z. Dong, Q. Fan, G. Zhang, H. Liu, Z. Li, Evolution and critical roles of particle properties in Pickering emulsion: a review, J. Mol. Liq. 388 (2023) 122775, https://doi.org/10.1016/j.molliq.2023.122775.
[2] L. Perrin, G. Gillet, L. Gressin, S. Desobry, Interest of Pickering emulsions for sustainable micro/nanocellulose in food and cosmetic applications, Polymers (Basel). 12 (2020) 2385, https://doi.org/10.3390/polym12102385.
[3] E. Viennois, B. Chassaing, Consumption of select dietary emulsifiers exacerbates the development of spontaneous intestinal adenoma, Int. J. Mol. Sci. 22 (2021) 2602, https://doi.org/10.3390/ijms22052602.
[4] C. Albert, M. Beladjine, N. Tsapis, E. Fattal, F. Agnely, N. Huang, Pickering emulsions: preparation processes, key parameters governing their properties and potential for pharmaceutical applications, J. Control. Release 309 (2019) 302–332, https://doi.org/10.1016/j.jconrel.2019.07.003.
[5] R.I. Dekker, S.F. Velandia, H.V.M. Kibbelaar, A. Morcy, V. Sadtler, T. Roques-Carmes, J. Groenewold, W.K. Kegel, K.P. Velikov, D. Bonn, Is there a difference between surfactant-stabilised and Pickering emulsions? Soft Matter 19 (2023) 1941–1951, https://doi.org/10.1039/D2SM01375D.
[6] Y. Chevalier, M.-A. Bolzinger, Emulsions stabilized with solid nanoparticles: Pickering emulsions, Colloids Surfaces A Physicochem. Eng. Asp. 439 (2013) 23–34, https://doi.org/10.1016/j.colsurfa.2013.02.054.
[7] Y. Li, D. Yang, S. Wang, H. Xu, P. Li, Fabrication and optimization of Pickering emulsion stabilized by lignin nanoparticles for curcumin encapsulation, ACS Omega 9 (2024) 21994–22002, https://doi.org/10.1021/acsomega.3c10395.
[8] O. Gordobil, N. Blažević, M. Simonič, A. Sandak, Potential of lignin multifunctionality for a sustainable skincare: impact of emulsification process parameters and oil-phase on the characteristics of O/W Pickering emulsions, Int. J. Biol. Macromol. 233 (2023), https://doi.org/10.1016/j.ijbiomac.2023.123561.
[9] J. Tian, J. Chen, P. Wang, J. Guo, W. Zhu, M.R. Khan, Y. Jin, J. Song, O.J. Rojas, Interfacial activity and Pickering stabilization of kraft lignin particles obtained by solvent fractionation, Green Chem. 25 (2023) 3671–3679, https://doi.org/10.1039/D3GC00692A.
[10] J. Tian, J. Chen, J. Guo, W. Zhu, M.R. Khan, Q. Fu, Y. Jin, H. Xiao, J. Song, O. J. Rojas, Pickering emulsions produced with kraft lignin colloids destabilized by in situ pH shift: effect of emulsification energy input and stabilization mechanism,

Colloids Surfaces A Physicochem. Eng. Asp. 670 (2023) 131503, https://doi.org/10.1016/j.colsurfa.2023.131503.
[11] M.R.V. Bertolo, L.B. Brenelli de Paiva, V.M. Nascimento, C.A. Gandin, M.O. Neto, C.E. Driemeier, S.C. Rabelo, Lignins from sugarcane bagasse: renewable source of nanoparticles as Pickering emulsions stabilizers for bioactive compounds encapsulation, Ind. Crop. Prod. 140 (2019) 111591, https://doi.org/10.1016/j.indcrop.2019.111591.
[12] K. Wang, M. Zhu, Z. Yang, L. Bai, S. Huan, C. Wang, Sustainable production of stable lignin nanoparticle-stabilized Pickering emulsions via cellulose nanofibril-induced depletion effect, ACS Sustain. Chem. Eng. 11 (2023) 9132–9142, https://doi.org/10.1021/acssuschemeng.3c01972.
[13] M. Yu, H. Xin, D. He, C. Zhu, Q. Li, X. Wang, J. Zhou, Electrospray lignin nanoparticles as Pickering emulsions stabilizers with antioxidant activity, UV barrier properties and biological safety, Int. J. Biol. Macromol. 238 (2023) 123938, https://doi.org/10.1016/j.ijbiomac.2023.123938.
[14] L. Chen, Y. Shi, B. Gao, Y. Zhao, Y. Jiang, Z. Zha, W. Xue, L. Gong, Lignin nanoparticles: green synthesis in a γ-valerolactone/water binary solvent and application to enhance antimicrobial activity of essential oils, ACS Sustain. Chem. Eng. 8 (2020) 714–722, https://doi.org/10.1021/acssuschemeng.9b06716.
[15] K. Gao, J. Liu, X. Li, H. Gojzewski, X. Sui, G.J. Vancso, Lignin nanoparticles as highly efficient, recyclable emulsifiers for enhanced oil recovery, ACS Sustain. Chem. Eng. 10 (2022) 9334–9344, https://doi.org/10.1021/acssuschemeng.2c01101.
[16] C.E. de A. Padilha, C. da C. Nogueira, S.C.B. Matias, J.D.B. da Costa Filho, D.F. de S. Souza, J.A. de Oliveira, E.S. dos Santos, Fabrication of hollow polymer microcapsules and removal of emulsified oil from aqueous environment using soda lignin nanoparticles, Colloids Surfaces A Physicochem. Eng. Asp. 603 (2020) 125260, https://doi.org/10.1016/j.colsurfa.2020.125260.
[17] K. Chen, Y. Qian, C. Wang, D. Yang, X. Qiu, B.P. Binks, Tumor microenvironment-responsive, high internal phase Pickering emulsions stabilized by lignin/chitosan oligosaccharide particles for synergistic cancer therapy, J. Colloid Interface Sci. 591 (2021) 352–362, https://doi.org/10.1016/j.jcis.2021.02.012.
[18] H. Cuthill, C. Elleman, T. Curwen, B. Wolf, Colloidal particles for Pickering emulsion stabilization prepared via antisolvent precipitation of lignin-rich cocoa shell extract, Foods 10 (2021) 371, https://doi.org/10.3390/foods10020371.
[19] G. Colucci, A. Santamaria-Echart, S.C. Silva, L.G. Teixeira, A. Ribeiro, A. E. Rodrigues, M.F. Barreiro, Development of colloidal lignin particles through particle design strategies and screening of their Pickering stabilizing potential, Colloids Surfaces A Physicochem. Eng. Asp. 666 (2023) 131287, https://doi.org/10.1016/j.colsurfa.2023.131287.
[20] C. Hadjiefstathiou, A. Manière, J. Attia, F. Pion, P.-H. Ducrot, E. Gore, M. Grisel, Lignins emulsifying properties according to pH to control their behavior at oil–water interface, J. Mol. Liq. 390 (2023) 123030, https://doi.org/10.1016/j.molliq.2023.123030.
[21] T.E. Nypelö, C.A. Carrillo, O.J. Rojas, Lignin supracolloids synthesized from (W/O) microemulsions: use in the interfacial stabilization of Pickering systems and organic carriers for silver metal, Soft Matter 11 (2015) 2046–2054, https://doi.org/10.1039/c4sm02851a.
[22] N. Ghavidel, P. Fatehi, Pickering/non-Pickering emulsions of nanostructured sulfonated lignin derivatives, ChemSusChem 13 (2020) 4567–4578, https://doi.org/10.1002/cssc.202000965.
[23] R. Shorey, T.H. Mekonnen, Esterification of lignin with long chain fatty acids for the stabilization of oil-in-water Pickering emulsions, Int. J. Biol. Macromol. 230 (2023) 123143, https://doi.org/10.1016/j.ijbiomac.2023.123143.
[24] W.D.H. Schneider, A.J.P. Dillon, M. Camassola, Lignin nanoparticles enter the scene: a promising versatile green tool for multiple applications, Biotechnol. Adv. 47 (2021) 107685, https://doi.org/10.1016/j.biotechadv.2020.107685.
[25] M. Österberg, M.H. Sipponen, B.D. Mattos, O.J. Rojas, Spherical lignin particles: a review on their sustainability and applications, Green Chem. 22 (2020) 2712–2733, https://doi.org/10.1039/D0GC00096E.
[26] M.H. Sipponen, H. Lange, M. Ago, C. Crestini, Understanding lignin aggregation processes. A case study: budesonide entrapment and stimuli controlled release from lignin nanoparticles, ACS Sustain. Chem. Eng. 6 (2018) 9342–9351, https://doi.org/10.1021/acssuschemeng.8b01652.
[27] T. Leskinen, M. Smyth, Y. Xiao, K. Lintinen, M. Mattinen, M.A. Kostiainen, P. Oinas, M. Österberg, Scaling up production of colloidal lignin particles - OPEN ACCESS, Nord. Pulp Pap. Res. J. 32 (2017) 586–596, https://doi.org/10.3183/NPPRJ-2017-32-04-p586-596.
[28] S. Cailotto, M. Gigli, M. Bonini, F. Rigoni, C. Crestini, Sustainable strategies in the synthesis of lignin nanoparticles for the release of active compounds: a comparison, ChemSusChem 13 (2020) 4759–4767, https://doi.org/10.1002/cssc.202001140.
[29] P.K. Mishra, A. Ekielski, The self-assembly of lignin and its application in nanoparticle synthesis: a short review, Nanomaterials 9 (2019) 243, https://doi.org/10.3390/nano9020243.
[30] T. Zou, E. Kimiaei, Z. Madani, M.A. Karaaslan, J. Vapaavuori, J. Foster, S. Renneckar, M. Österberg, Hydrophobized lignin nanoparticle-stabilized Pickering foams: building blocks for sustainable lightweight porous materials, Mater. Adv. 5 (2024) 5802–5812, https://doi.org/10.1039/D4MA00295D.
[31] J. Tian, J. Chen, P. Wang, S. Kang, J. Guo, W. Zhu, Y. Jin, J. Song, O.J. Rojas, Pickering emulsion stabilization with colloidal lignin is enhanced by salt-induced networking in the aqueous phase, Int. J. Biol. Macromol. 274 (2024) 133504, https://doi.org/10.1016/j.ijbiomac.2024.133504.
[32] L. Wang, Y. Kang, W. Zhang, J. Yang, H. Li, M. Niu, Y. Guo, Z. Wang, Preparation of lignin-based nanoparticles with excellent acidic tolerance as stabilizer for Pickering emulsion, Polymers (Basel) 15 (2023) 4643, https://doi.org/10.3390/polym15244643.
[33] G. Colucci, M. Gigli, M. Sgarzi, A.E. Rodrigues, C. Crestini, M.F. Barreiro, Modulation of physicochemical and antioxidant properties of Pickering emulsions using colloidal lignin particles based on kraft softwood and hardwood acetone fractions, Sep. Purif. Technol. 347 (2024) 127570, https://doi.org/10.1016/j.seppur.2024.127570.
[34] S. Bertella, M. Bernardes Figueirêdo, G. De Angelis, M. Mourez, C. Bourmaud, E. Amstad, J.S. Luterbacher, Extraction and surfactant properties of glyoxylic acid-functionalized lignin, ChemSusChem 15 (2022), https://doi.org/10.1002/cssc.202200270.
[35] A. Boarino, J. Charmillot, M.B. Figueirêdo, T.T.H. Le, N. Carrara, H.-A. Klok, Ductile, high-lignin-content thermoset films and coatings, ACS Sustain. Chem. Eng. 11 (2023) 16442–16452, https://doi.org/10.1021/acssuschemeng.3c03030.
[36] F.M.C. Freitas, M.A. Cerqueira, C. Gonçalves, S. Azinheiro, A. Garrido-Maestu, A. A. Vicente, L.M. Pastrana, J.A. Teixeira, M. Michelin, Green synthesis of lignin nano- and micro-particles: physicochemical characterization, bioactive properties and cytotoxicity assessment, Int. J. Biol. Macromol. 163 (2020) 1798–1809, https://doi.org/10.1016/j.ijbiomac.2020.09.110.
[37] A. Sharkawy, M.F. Barreiro, A.E. Rodrigues, Preparation of chitosan/gum arabic nanoparticles and their use as novel stabilizers in oil/water Pickering emulsions, Carbohydr. Polym. 224 (2019) 115190, https://doi.org/10.1016/j.carbpol.2019.115190.
[38] M. Lievonen, J.J. Valle-Delgado, M.-L. Mattinen, E.-L. Hult, K. Lintinen, M. A. Kostiainen, A. Paananen, G.R. Szilvay, H. Setälä, M. Österberg, A simple process for lignin nanoparticle preparation, Green Chem. 18 (2016) 1416–1422, https://doi.org/10.1039/C5GC01436K.
[39] S. Beisl, P. Loidolt, A. Miltner, M. Harasek, A. Friedl, Production of micro- and nanoscale lignin from wheat straw using different precipitation setups, Molecules 23 (2018) 633, https://doi.org/10.3390/molecules23030633.
[40] B.P. Binks, Particles as surfactants—similarities and differences, Curr. Opin. Colloid Interface Sci. 7 (2002) 21–41, https://doi.org/10.1016/S1359-0294(02)00008-0.
[41] D.J. McClements, J. Lu, L. Grossmann, Proposed methods for testing and comparing the emulsifying properties of proteins from animal, plant, and alternative sources, Colloids and Interfaces. 6 (2022) 19, https://doi.org/10.3390/colloids6020019.
[42] A. Ribeiro, Y.A. Manrique, F. Barreiro, J.C.B. Lopes, M.M. Dias, Continuous production of hydroxyapatite Pickering emulsions using a mesostructured reactor, Colloids Surfaces A Physicochem. Eng. Asp. 616 (2021) 126365, https://doi.org/10.1016/j.colsurfa.2021.126365.
[43] C. Frangville, M. Rutkevičius, A.P. Richter, O.D. Velev, S.D. Stoyanov, V. N. Paunov, Fabrication of environmentally biodegradable lignin nanoparticles, ChemPhysChem 13 (2012) 4235–4243, https://doi.org/10.1002/cphc.201200537.
[44] B.P. Binks, J.H. Clint, Solid wettability from surface energy components: relevance to Pickering emulsions, Langmuir 18 (2002) 1270–1273, https://doi.org/10.1021/la011420k.
[45] G. Kaptay, On the equation of the maximum capillary pressure induced by solid particles to stabilize emulsions and foams and on the emulsion stability diagrams, Colloids Surfaces A Physicochem. Eng. Asp. 282–283 (2006) 387–401, https://doi.org/10.1016/j.colsurfa.2005.12.021.
[46] H. Kumar, S. Upendar, E. Mani, Madivala G. Basavaraj, Destabilization of Pickering emulsions by interfacial transport of mutually soluble solute, J. Colloid Interface Sci. 633 (2023) 166–176, https://doi.org/10.1016/j.jcis.2022.10.133.
[47] X. Li, J. Shen, B. Wang, X. Feng, Z. Mao, X. Sui, Acetone/water cosolvent approach to lignin nanoparticles with controllable size and their applications for Pickering emulsions, ACS Sustain. Chem. Eng. 9 (2021) 5470–5480, https://doi.org/10.1021/acssuschemeng.1c01021.
[48] A. Ribeiro, Y.A. Manrique, I.C.F.R. Ferreira, M.F. Barreiro, J.C.B. Lopes, M.M. Dias, Nanohydroxyapatite (n-HAp) as a Pickering stabilizer in oil-in-water (O/W) emulsions: a stability study, J. Dispers. Sci. Technol. 43 (2020) 814–826, https://doi.org/10.1080/01932691.2020.1845199.
[49] J. Ding, Y. Li, Q. Wang, L. Chen, Y. Mao, J. Mei, C. Yang, Y. Sun, Pickering high internal phase emulsions with excellent UV protection property stabilized by Spirulina protein isolate nanoparticles, Food Hydrocoll. 137 (2023) 108369, https://doi.org/10.1016/j.foodhyd.2022.108369.
[50] D.E. Tambe, M.M. Sharma, The effect of colloidal particles on fluid-fluid interfacial properties and emulsion stability, Adv. Colloid Interf. Sci. 52 (1994) 1–63, https://doi.org/10.1016/0001-8686(94)80039-1.
[51] M.N. Lee, H.K. Chan, A. Mohraz, Characteristics of Pickering emulsion gels formed by droplet bridging, Langmuir 28 (2012) 3085–3091, https://doi.org/10.1021/la203384f.
[52] D.J. French, P. Taylor, J. Fowler, P.S. Clegg, Making and breaking bridges in a Pickering emulsion, J. Colloid Interface Sci. 441 (2015) 30–38, https://doi.org/10.1016/j.jcis.2014.11.032.
[53] T.G. Mezger, Applied Rheology, Anton Paar GmbH, Graz, Austria, 2015.
[54] D. Pinto, F. Lameirão, C. Delerue-Matos, F. Rodrigues, P. Costa, Characterization and stability of a formulation containing antioxidants-enriched Castanea sativa shells extract, Cosmetics 8 (2021) 49, https://doi.org/10.3390/cosmetics8020049.
[55] L. Gilbert, C. Picard, G. Savary, M. Grisel, Rheological and textural characterization of cosmetic emulsions containing natural and synthetic polymers: relationships between both data, Colloids Surfaces A Physicochem. Eng. Asp. 421 (2013) 150–163, https://doi.org/10.1016/j.colsurfa.2013.01.003.